Preparation of Magnetic Cellulose Nanocrystal -Modified Diatomite for Removal of Methylene Blue from Aqueous Solutions

Hunan, Liang*[+•]***; Xiao, Hu***

School of Chemical Engineering, Northeast Electric Power University,
168 Changchun Road, Jilin, 132102, P R. CHINA

ABSTRACT: *The Magnetic Cellulose Nanocrystal-Modified Diatomite (MCNCD) composite was synthesized and its adsorption performance for removal of Methylene Blue (MB) dye from aqueous solutions was investigated. The as-prepared MCNCD samples were characterized by Fourier transform infrared spectroscopy, scanning electron microscopy, thermal gravimetric analyzer, and vibration sample magnetometer, respectively. The adsorption parameters such as temperature, initial concentration of MB, adsorption time, and pH, were studied. The adsorption isotherms and kinetics were established. The results showed that adsorption isotherm and kinetics fitted well to the Langmuir model and pseudo-second-order model, respectively. Furthermore, the as-prepared MCNCD samples can be reused/ recycled after regeneration, with an adsorption capacity of 46.21 mg/g after six cycles.*

KEYWORDS: *Magnetism; Cellulose nanocrystal; Modification; Diatomite; Methylene blue; Adsorption.*

INTRODUCTION

Organic dyes are widely applied in many industries such as textile, leather, printing, and papermaking. Annually, large amounts of these dyes are discharged from manufacturing operations resulting in colored wastewater [1], Dye is very difficult to be treated/ degraded in wastewater treatment systems [2], which can cause harmful effects on the human body and environment[1, 3-4]. Therefore, the effective removal/ degradation of these dyes from wastewater has been a popular topic in the research community. Different approaches such as flocculation [5, 6], membrane [7-10], oxidation [11-13], Electro-coagulation [14], catalysis [15, 16], and adsorption [17-22], have been studied. Among them, adsorption is considered to be a competitive and effective method on account of its low cost, easy operation, environmental friendliness, and non-toxicity [20-22]. Various low-cost adsorbents were developed for this purpose. In recent years, natural materials as adsorbents, have received much attention due to their renewability, biodegradability, nontoxicity, and eco-friendliness [20, 21].

***** *To whom correspondence should be addressed.*
+ *E-mail*: *lianghunan202@163.com*
● *Other Address: School of Chemical Engineering, Northeast Electric Power University, Changchun road, Jilin , Jilin, 132012, P.R. CHINA*
1021-9986/2022/3/787-798 *12/$/6.02*

INTRODUCTION

Diatomite is an inorganic material with low cost, high porosity, low density, and chemical/ biochemical stability [22, 23]. Diatomite has been studied as an adsorbent for removing pollutants from wastewater [24, 25]. The performance of natural diatomite as an effective absorbent for dyes is limited due to the presence of its impurities and inferior adsorption sites on the surface [26, 27]. Further modifications of diatomite can enhance its adsorption properties [28, 29]. For example, organic modification can improve the performance and utility of inorganic materials [29]. Cellulose NanoCrystal (CNC), as organic material from nature, can be extracted from lignocellulosic materials [30-32], and CNC can be used in wastewater treatment because of its adsorptive property and electrostatic interactions involving hydroxyl groups [31]. Similarly, magnetic materials are desirable as adsorbents to treat water contamination [33-34], because it is convenient to separate the adsorbents after use from an aqueous solution under the external magnetic field so that they can be reused/ recycled [35].

In this study, natural diatomite was first modified with CNC, then made magnetic by adding ferric chloride and ferrous sulfate, resulting in the formation of Magnetic Cellulose NanoCrystal-modified Datomite Composite (MCNCD). Subsequently, the potential of the as-prepared MCNCD as an effective adsorbent for the removal of cationic dye (methylene blue, MB, as a model) was evaluated. The regeneration/recycling of MCNCD for MB adsorption was also investigated.

EXPERIMENTAL SECTION

Materials

The CNC was purchased from Tianjin Haojia Cellulose nanocrystal Co., Ltd., China. The diatomite was supplied from Jilin Yuantong Mining Co., Ltd., China.

Ferric chloride hexahydrate and ferrous sulfate heptahydrate were purchased from Shenyang East China reagents Co., China. Sodium hydroxide was purchased from Tianjin Damao Chemical Industry, China. Methylene blue was purchased from Shenyang Third Reagents Co., China. Sulfuric acid was purchased from Yantai Shuangshuang Chemical Industry Co., Ltd., China. All reagents were reagent grade and were used without further purification.

Synthesis of Magnetic Cellulose NanoCrystal-modified Diatomite (MCNCD)

The preparation of MCNCD was described according to the previous works [17, 36] with minor modifications. First, CNC suspensions were prepared using 0.5 g of CNC dispersed in 500 mL deionized water and ultrasonic treatment for 30 min. Then, 0.5 g of dry diatomite was added to the CNC suspensions under the condition of pH 7, 60℃, and magnetically stirred for 3 h. Subsequently, it was centrifuged and washed several times with deionized water until a constant pH was reached. After that, the obtained Cellulose NanoCrystal-modified Diatomite (CNCD) was dried for further usage.

Magnetic Modified Cellulose NanoCrystal-modified Diatomite (MCNCD) composite was synthesized as follows. 1g CNCD was dispersed in 100ml deionized water. 0.27g ferric chloride hexahydrate and 0.28g ferrous sulfate heptahydrate were successively added to the CNCD suspension in a nitrogen atmosphere and stirred at ambient temperature for 30 minutes. Then sodium hydroxide (was dropped into suspension to maintain the pH 10. Afterward, the black sediments were washed with deionized water and ethyl alcohol alternately until pH 0.1M) maintain constant. Finally, the composite was dried in a vacuum at 60 ℃ for 12 hours.

Characterization

The chemical composition of the samples was determined by Fourier Transform InfraRed spectrum (FT-IR, IRAffinity-1, Japan). The TGA curves were obtained using a Q600 machine (TA Instruments, USA) in the temperature range of 25 to 600 ℃ at a heating rate of 10 ℃ /min under nitrogen flow. X-Ray Diffraction (XRD) pattern of samples was obtained on a Bruker D8 Advance spectrometer (XRD-7000s, Shimadzu, Japan). Morphology of samples was examined using a Scanning Electron Microscope (SEM, JSM-7610F, Jeol, Japan), Thermal Gravimetric Analyzer (TGA, DACI-TGA, Mettler Toledo, Switzerland), and vibration sample magnetometer (VSM, HH-12, China) were used to determine the structure of samples and the magnetic saturation of MCNCD.

Adsorption Experiments

Effect of adsorption temperature

The adsorption experiments were performed in a conical flask by contacting 0.005g MCNCD with 30mL of 20mg/L MB dye solution. The conical flask was sealed and left on a thermostatic shaker at 25°C, 30°C, 35°C, 40°C, 50°C, respectively. Samples of 5mL were taken from the solution after 420 min to determine adsorption capacity.

Effect of initial pH

The initial pH values were adjusted to the target one in a range of 3.0 to 11.0 using 0.1M NaOH or HCl solutions as required. 5mL solutions of the sample were extracted from the suspension on a pre-set schedule (420 min) to determine the adsorption capacity.

Adsorption kinetic study experiments

Adsorption kinetic experiments were performed at 20mg/L of initial MB concentration and the adsorption amount of dye by MCNCD was measured at pre-set time intervals ranging from 5-700min. Samples of 5mL were taken from the solution after 420 min to determine adsorption capacity.

Adsorption isotherm study experiments

Adsorption isotherm experiments were conducted with various initial MB concentrations (c_0=20-800mg/L) for 420 min. Samples of 5mL were taken from the solution after 420 min to determine adsorption capacity.

Analytical methods

The adsorption amount at the equilibrium (q_e, mg/g) was calculated by following Eq. (1).

$$q_e = \frac{(c_0 - c_e)v}{m} \quad (1)$$

Where c_0 and c_e are the initial and equilibrium MB concentration (mg/L), respectively. v is the volume of solution (L) and m is the amount of adsorbent (g).

The adsorption experiments were based on OFAT approach. And the experimental data were statistically analyzed with one-way Analysis of Variance (ANOVA) using Statistical Package for Social Sciences (SPSS) software for the effect of different factors on the MB adsorption by MCNCD. $P<0.05$ is considered significant.

Regeneration experiments

Regeneration of the MCNCD adsorbent was conducted as follows: the MCNCD was separated using a magnet and dried after the adsorption experiment. The dried sample was added to a conical flask with 1 mol/L HCl solution, and the flask with its contents was placed on a platform-shaker for 48h (25 °C). Subsequently, the sample was washed with ethanol in a centrifuge a few times until the supernatant was neutral. Finally, the recycled MCNCD sample was separated and dried in a vacuum box.

The regenerated MCNCD was reused to adsorb MB in an aqueous solution under the same optimal conditions. Samples of 5mL were taken from the solution after 420 min to determine adsorption capacity.

RESULTS AND DISCUSSION

Characterization

The FT-IR spectra of CNC, diatomite, and MCNCD were presented in Fig.1. A strong peak for CNC and MCNCD at 3344 and 3348 were related to the O-H group and, peaks at 2901cm-1 and 2899 cm-1 were due to the C-H stretching of cellulose. In the spectrum of MCNCD, a strong peak of 798 cm^{-1} and 1033 cm^{-1} were detected, which was produced by the joint action of Si-O-Si in diatomite [37].

The adsorption peak of MCNCD at 702 cm^{-1} is the Fe-O band in Fe_3O_4. The above results support the conclusion that the Magnetic Cellulose NanoCrystal/Diatomite (MCNCD) composite was synthesized successfully.

XRD patterns of CNC, diatomite, and MCNCN were shown in Fig.2. The XRD pattern of CNC displayed four characteristic peaks of crystalline nature of cellulose I 2θ at 14.9°, 16.5°, 22.8°, corresponding to the diffraction planes of (1$\underline{1}$0), (110), and (020), respectively [38]. Two wide peaks were shown at 21.8° and 36.1° for diatomite, characteristics of SiO_2 [39]. In addition, the peaks occurring at 2θ of 30.1°, 35.4°, 43.1°, 56.9°, 62.5° showed that the prepared MCNCD had pure Fe_3O_4 with spinel structure [40]. The XRD patterns confirmed the existence of CNC, diatomite, and Fe_3O_4 in the MCNCD composite.

SEM measurement was used for characterizing the microscopic structure of samples. The SEM images of samples are shown in Fig.3. Fig. 3 (a) was TEM image of CNC supplied by Tianjin Haojiao co. ltd. The spindle morphology of CNC was shown in TEM image. For diatomite morphology, the porous structure of pure diatomite was obviously presented in Fig. 3 (b). By comparison, the CNC with a spindle covered on a diatomite surface can be seen in the enlargement of SEM image in Fig. 3 (c), illustrating CNC attached to the surface of diatomite. This was shown that the CNC was successfully composited with diatomite. Furthermore, it is easy to find that magnetic material dispersed in CNCD from SEM image of the MCNCD (Fig. 3 (d)).

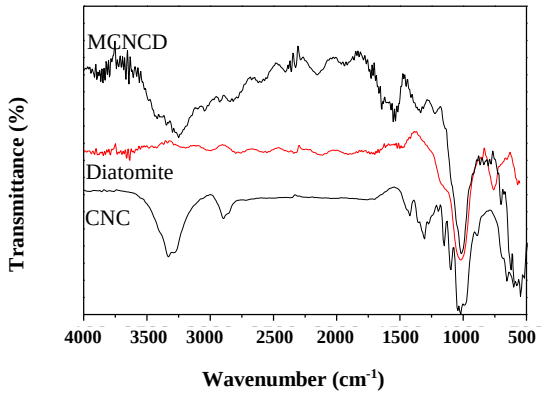

Fig. 1: FTIR spectra of CNC, Diatomite and MCNCD.

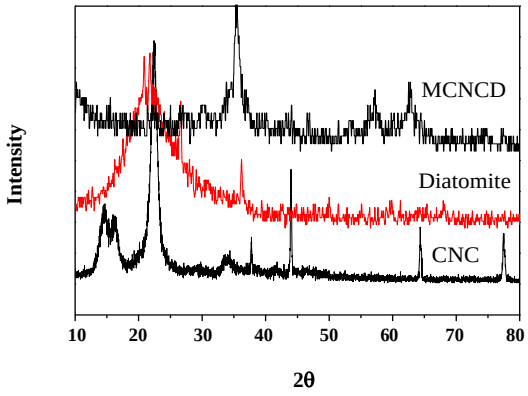

Fig. 2: XRD patterns of CNC, Diatomite and MCNCD.

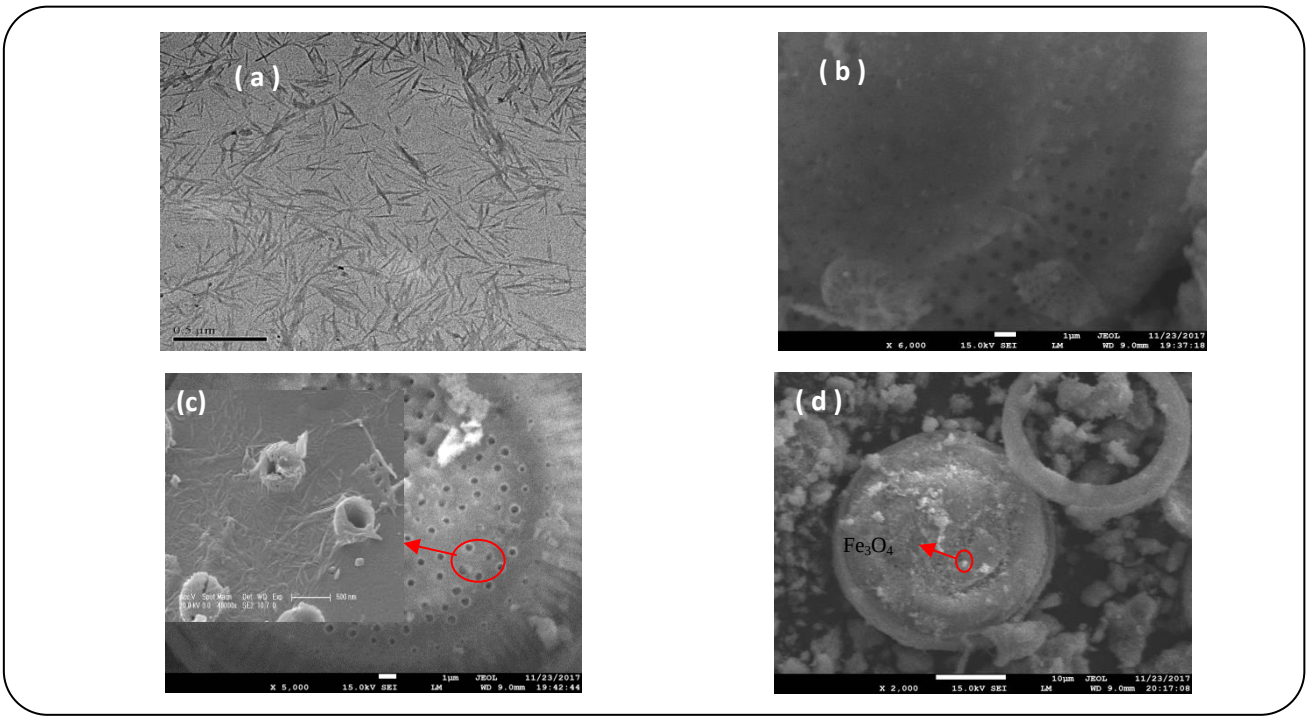

Fig. 3: TEM photograph of CNC (a), SEM photographs of Diatomite (b), CNCD (c) and MCNCD (d).

TGA is an important tool for detecting the thermal stability of materials. The TGA curves of CNC, diatomite, and MCNCD are given in Fig. 4. The TGA curve of diatomite showed a slight mass loss of about 3%, which was mainly due to the evaporation of water and decomposition of some impurities. For CNC, there were three stages of mass losses in the range of 20-600℃. In the first stage, an initial small weight loss of about 10% between 20 °C and 200 °C corresponded to absorbed moisture. The second stage and third stage were in the range of 200-350 °C and 350-600℃ with weight loss of 55% and 35%, respectively, which attributed to CNC thermal degradation. The TGA thermograms of the MCNCD showed that there were three steps for thermal degradation of the samples, the first degradation (20-300 °C) characterized the loss of moisture in samples with approximately 5% of mass loss. The maximum values of mass loss for MCNCD with about 17% mass occurred in the second stage of 200–350 °C, which were mainly related to the degradation of CNC. The third stage above 350 °C was related to CNC degradation, the mass of MCNCD was nearly unchanged. The results obtained

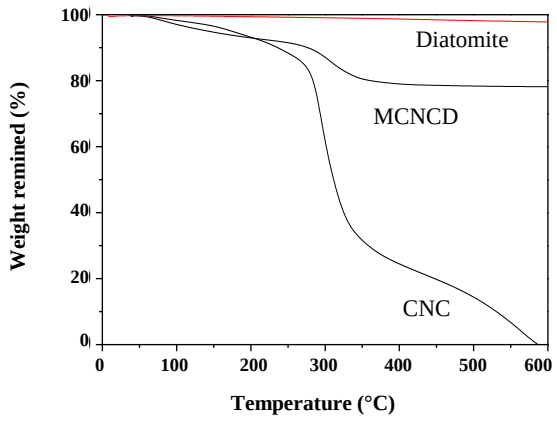

Fig. 4: TGA curves of cellulose, diatomite, and MCNCD.

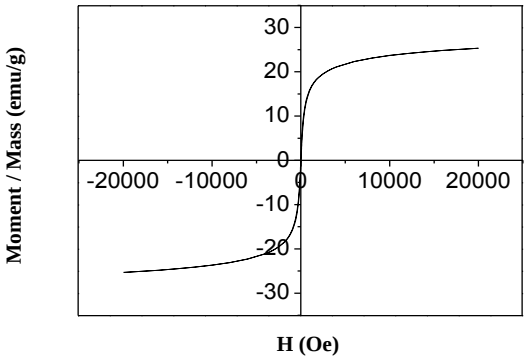

Fig. 5. Hysteresis loops of the MCNCD sample at room temperature.

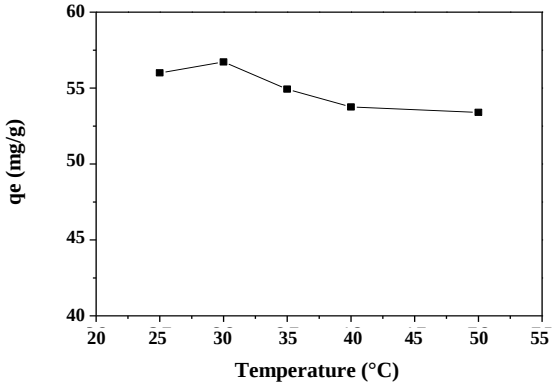

Fig. 6. Effect of temperature on the adsorption capacity of the MCNCD for MB.

in TGA confirms magnetic ferroferric oxide in the prepared MCNCD.

The magnetic property of the MCNCD was characterized by a Vibrating Sample Magnetometer (VSM) at room temperature (25℃), and the results are presented in Fig. 5. It was shown that the saturation magnetization of the MCNCD was 25.3 emu/g at the applied magnetic field of 20000 Oe, showing a strong magnetic response for the magnetic field. The results demonstrated that the MCNCD can be used as an adsorbent for removing MB from the aqueous medium, subsequently, it can be recovered/reused by using a magnetic field.

Adsorption

Effect of temperature

The effect of temperature on MB removal by MCNCD is presented in Fig. 6. The effect of temperature on MB adsorbed onto MCNCD is small. The small increase in adsorption capacity is due to the improvement of the rate at that MB molecules diffuse into polyporous MCNCD due to the decrease in the viscosity of the solution with the temperature increasing [41]. The reduction of adsorption capacity from 30 to 50ºC may be attributed to the exothermic nature of the adsorption process. The maximum adsorption capacity appeared at 30 ºC, so further adsorption experiments were conducted at 30 ºC.

Effect of pH

The pH of the solution can distinctly affect the adsorption capacity of MB from an aqueous medium [42]. The results of the effect of pH on the removal of MB are shown in Fig.7. It was clear from the diagram that, the adsorption capacity of MB increased with increasing pH, it was increased from 31.7 mg/g to 60 mg/g with an increase in the pH from 3 to 9. The adsorption efficiency was in significant when pH increased above 9. This variation tendency was in accordance with the literature [43]. MB was adsorbed onto MCNCD because of the electrostatic reaction between the cationic MB dye and the negative hydroxyl groups on CNC and diatomite. The surface of MCNCD is more negatively charged with increasing the pH of the medium, so the electrostatic interactions between MB and negative groups of MCNCD increase and facilitate MB adsorption. The adsorption capacity equilibrated after pH 9; therefore, pH 9 was used in the next adsorption experiments.

Adsorption kinetics

Adsorption is a physicochemical phenomenon, which encompasses the mass transfer of a solute from the solution

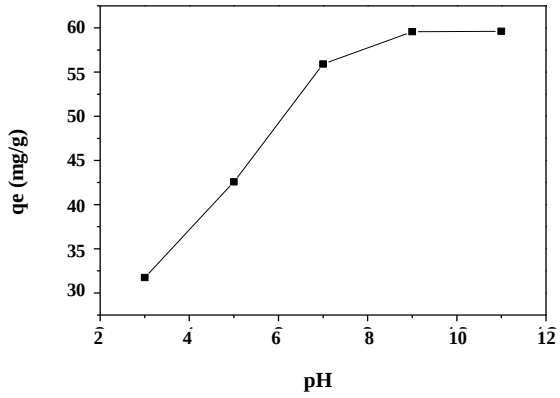

Fig. 7: Effect of pH on the adsorption capacity of the MCNCD for MB.

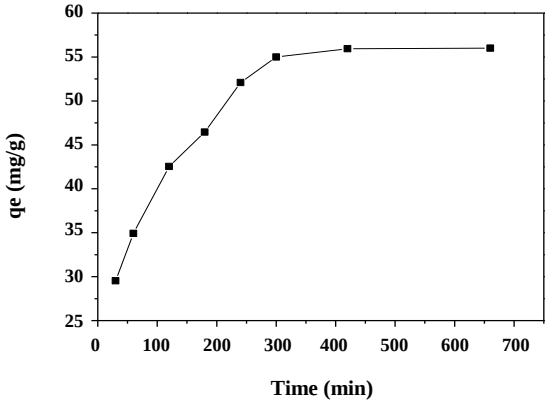

Fig. 8: Effect of time on the adsorption capacity of the MCNCD for MB.

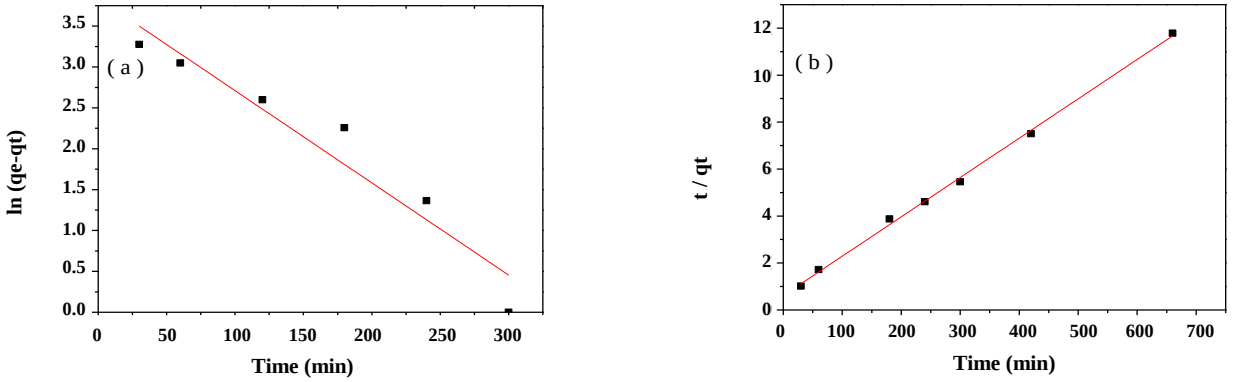

Fig. 9: Pseudo-first (a) and second (b) kinetics modeling MB adsorption.

to the adsorbent. The effect of time on the adsorption of MB onto MCNCD is shown in Fig. 8. It can be seen that the capacity of adsorption for MB increased with contact time and the maximum adsorption capacity reached 56 mg/g. The adsorption amounts increased when extending the time, as a result of more adsorption of MB molecules onto the MCNCD structure. Then adsorption rate gradually decreases because of the gradual saturation of all active sites of MCNCD by MB molecules [44]. The experiment results showed that adsorption capacity reached equilibrium after 300min, so further adsorption experiments were performed for 300min.

The adsorption data were fitted using the pseudo-first-order and pseudo-second-order kinetic models for further investigating the adsorption process and mechanism. The pseudo-second-order kinetic curve showed in Fig. 9.

Pseudo-first and second-order models, which can define the mechanism of adsorption, were used for characterizing the MB adsorption progress by MCNCD.

The linearized pseudo-first-order equations are expressed as Eq. (2) [45]:

$$\ln\left(q_e - q_t\right) = \ln q_e - K_1 t \quad (2)$$

Where q_t and q_e represent the adsorption capacity of MB at time t and equilibrium (mg/g), respectively. K_1 is the pseudo-first-order rate constant (min^{-1}).

The linearized pseudo-second-order equations are expressed as (3) :

$$\frac{t}{q_t} = \frac{t}{q_e} + \frac{1}{K_2 q_e^2} \quad (3)$$

Where q_t and q_e represent the removal capacity of MB at time t and equilibrium (mg/g) respectively. K_2 is the pseudo-second-order rate constant (g/ mg.min).

Table 1: Kinetics modeling of MB adsorption progress.

Temperature	Kinetics model	q_e(mg/g)	K_1(min^{-1})	K_2(g mg^{-1} min^{-1})	R^2
25℃	Pseudo-first-order	46.48	0.011	—	0.9104
	Pseudo-second-order	100	—	0.00016	0.9977

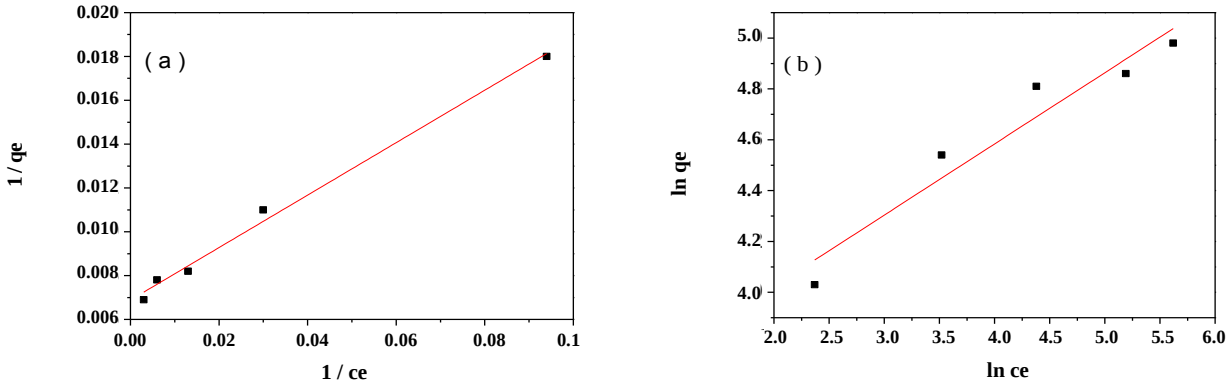

Fig. 10: Langmuir (a) and Freundlich isotherm model of MB removal.

The parameters of fitting results were exhibited in Fig. 9 and Table 1. As shown in Fig. 9 and Table 1, the MB adsorption of MCNCD fitted well to both pseudo-first-order and pseudo-second-order models, with all correlation coefficient values (R^2) being higher than 0.90. But the pseudo-second-order model fitted the test data better than that of the pseudo-first-order model, with R^2 value of 0.9977, indicating that chemical adsorption was the dominating adsorption. Similar results were reported in [46]. However, ammonium adsorption by biochars derived from biogas waste materials presented fit well with the Elovich model [47].

Adsorption isotherms

Adsorption isotherms can reflect the interaction between adsorbents and adsorbates. The Langmuir and Freundlich adsorption isotherm models were used to analyze the mechanism of MCNCD adsorbed MB.

Langmuir adsorption isotherm model is given in Equation (4):

$$\frac{c_e}{q_t} = \frac{c_e}{q_{max}} + \frac{1}{\alpha q_{max}} \quad (4)$$

Where q_{max} is the maximum amount of adsorption (mg/g), α is isotherm constant (L/mg), c_e and q_e are the equilibrium solution concentration (mg/L), and equilibrium adsorption (mg/g).

Freundlich adsorption isotherm model is given in Equation (5):

$$\ln q_e = \ln K_F + \ln c_e / n \quad (5)$$

Where K_F evaluates the adsorption performance of adsorbent (mg/g), n is adsorption tension (L/mg), c_e and q_e are the equilibrium solution concentration (mg/L), and equilibrium adsorption (mg/g).

The fitting curves and fitting parameters of two isotherm models are presented in Fig.10 and Table 2, respectively. The results show that the correlation coefficient of the Langmuir model (R^2=0.9981) is higher than that of Freundlich (R^2=0.9272), indicating that the adsorbing MB action by MCNCD is monolayer adsorption, which is attributed to chemical adsorption, and the maximum MB adsorption capacity of MCNCD is 166.67 mg/g in theoretical value. Comparatively, the Freundlich model assumes that adsorption takes place in multilayer [48]. For multi-layer adsorption, the adsorption can be a multi-molecular layer due to existing a certain space of adsorption force field near the adsorbent surface, which belongs to physical adsorption.

Various adsorbents have been developed for the removal of MB from an aqueous solution. Therefore, it is necessary to compare MCNCD with other adsorbents applied for the adsorption of MB. The prepared samples showed a higher

Table 2: Isotherm models of MB adsorption progress.

Model	q_m (mg/g)	a (L/mg)	K_F	n	R^2
Langmuir	166.67	0.050	—	—	0.9917
Freundlich	—	—	32.07	3.57	0.9105

Table 3: Comparison of maximum adsorption capacities of different adsorbents for MB removal.

Adsorbent	Adsorption capacity (q_m. mg/g)	Reference
NH2-MWCNTs@Fe3O4	178.57	[43]
Nanocrystalline cellulose	101.16	[49]
Porous carbon monoliths	127.53	[49]
Activated lignin-chitosan	36.25	[50]
Chitosan/zeolite	24.00	[51]
Graphene oxide/Fe3O4	154.00	[52]
MWCNTs/Gly/β-CD	90.90	[53]
Tungsten oxide nanowire	188.00	[54]
Diatomite	27.86	[55]
Purified diatomite	105.03	[56]
MCNCD	166.67	Present work

adsorption capacity than other adsorbents reported in the literature, as shown in Table 3. The high adsorption ability of MCNCD could be attributed to the abundant hydroxyl groups existing in CNC and diatomite with negative charge properties, which can interact with cationic MB dye through strong electrostatic interaction. These results support the conclusion that the as-prepared MCNCD is a potential adsorbent for removing MB from an aqueous solution.

Statistical analysis

In order to estimate the effect efficiencies of different factors, experimental data were analyzed with one-way ANOVA using SPSS software. The experimental results were presented in Table 4.

One-way ANOVA explained obviously different adsorption capacities in the various factor. The analytical data were shown in Table 5. In Table 5, temperature showed the standard deviation (1.421), which represented obviously lower than that of the pH (12.321), initial concentration (34.899), and adsorption time (10.148) ($P<0.001$). The analytical results were consistent with experimental results, namely, the temperature had no significant effect on the adsorption of MB by MCNCD.

Regeneration experiments

To investigate the regeneration of adsorbent, the MCNCD was reused/recycled for a number of repeating cycles. The results showed that, after six cycles, the adsorption capacity of MCNCD was 82.5% of the original value (Fig. 11). Hence, we conclude that MCNCD has high adsorption capacity and can be reused/ recycled for MB adsorption, which makes it a cost-effective adsorbent for MB removal from an aqueous medium.

CONCLUSIONS

In this work, a Magnetic Cellulose NanoCrystal-modified Diatomite (MCNCD) composite was successfully synthesized, and subsequently characterized based on FTIR, XRD, SEM, TGA, and VSM techniques. The adsorption results of MCNCD for methylene blue dye support the conclusion that the as-prepared MCNCD can be effectively applied to remove cationic dyes from aqueous solutions. Adsorption kinetic studies showed that the adsorption process fitted the pseudo-second-order model and the adsorption isotherm well followed the Langmuir model. The MCNCD can be reused/ recycled. These results imply that the as-prepared MCNCD can be applied as a low-cost

Table 4: The results of adsorption experiment.

Factor		q_e(mg/g)
Temperature (℃)	25	56.00
	30	56.72
	35	54.93
	40	53.75
	50	53.40
pH	3	31.75
	5	42.58
	7	55.92
	9	59.57
	11	59.62
Initial concentration (mg/ L)	20	55.92
	50	93.73
	100	122.11
	200	128.56
	300	144.59
Adsorption time (min)	30	29.52
	60	34.92
	120	42.55
	180	46.45
	240	52.09
	300	55.00
	420	55.94
	660	56.00

Table 5: Difference in adsorption properties concerning various factors.

Factor	N	Mean±standard deviation
Temperature	5	54.9600±1.421
pH	5	49.8880±12.321
Initial concentration	5	108.9820±34.899
Adsorption time	8	46.5587±10.148

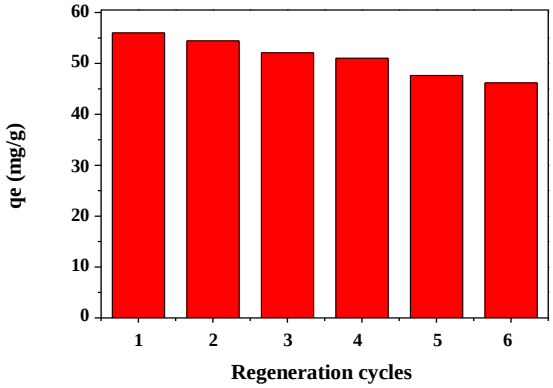

Fig. 11: Effect of regeneration frequencies on the adsorption capacity of the MCNCD for MB.

and efficient adsorbent for cationic dye removal from wastewater. Furthermore, as renewable lignocellulosic biomass, CNC would be widely applied as an inexpensive material for the pollution treatment of the environment.

Received : Oct. 12, 2020 ; Accepted : Jan. 4, 2021

REFERENCE

[1] Manikandan P., Palanisamy P.N., Baskar R., Sakthisharmila P., Sivakumar P., A Comparative Study on the Competitiveness of Photo-assisted Chemical Oxidation (PACO) with Electrocoagulation (EC) for the Effective Decolorization of Reactive Blue Dye, *Iran. J. Chem. Chem. Eng. (IJCCE)*, **36(1)**: 71-85 (2017).

[2] Bae W. Won H., Hwang B.Y., De Toledo R. A., Chung J.W., Kwon K., Shim H., Characterization of Refractory Matters in Dyeing Wastewater During a Full-Scale Fenton Process Following Pure-oxygen Activated Sludge Treatment, *J. Hazard. Mater.*, **287**: 421-428(2015).

[3] Eva Gnana Dhana Rani S., Ganesh Kumar A., Steplinpaulsevin S., Rajaram R., Tamil Selvan S., Sharmila Lydia L., Yong C., Survival Assessment of Simple Food Webs for Dye Wastewater after Photocatalytic Degradation Using SnO_2/GO Nanocomposites under Sunlight Irradiation, *Sci. total Environ.*, **721**:137805(2020).

[4] Thu H. N., Takahiro W., Masashi H., Dausike S., Tjandra S., Takashi Y., Evaluation of a Combined Anaerobic Baffled Reactor–downflow Hanging Sponge Biosystem for Treatment of Synthetic Dyeing Wastewater, *Environ. Technol. Inno.*, **19**: 100913 (2020).

[5] Wu H., Liu Z.Z., Li A.M., Yang H., Evaluation of Starch-Based Flocculants for the Flocculation of Dissolved Organic Matter from Textile Dyeing Secondary Wastewater, *Chemosphere*, **174:** 200-207(2017).

[6] Feng Q.Y., Gao B.Y., Yue Q.Y., Guo K.Y., Flocculation Performance of Papermaking Sludge-based Flocculants in Different Dye Wastewater Treatment: Comparison with Commercial Lignin and Coagulants, *Chemosphere*, **262**:128416(2020).

[7] Karim Z., Mathew A.P., Grahn M., Mouzon J., Oksman K., Nanoporous Membranes with Cellulose Nanocrystals as Functional Entity in Chitosan: Removal of Dyes from Water, *Carbohyd. Polym.*, **112**: 668-676(2014).

[8] Zeng G.Y., He Y., Zhan Y.Q., Zhang L., Pan Y., Zhang C.L., Yu Z.X., Novel Polyvinylidene Fluoride Nanofiltration Membrane Blended with Functionalized Halloysite Nanotubes for Dye and Heavy Metal Ions Removal, *J. Hazard. Mater.*, **317(5)**: 60-72(2016).

[9] Sun M., Yan L.L., Zhang L.H., Song L.F., Guo J.G., Zhang H. F., New Insights into the Rapid Formation of Initial Membrane Fouling after *In-Situ* Cleaning in a Membrane Bioreactor, *Process Biochem.*, **78:** 108-113(2019).

[10] Song Y.H., Seo J.Y., Kim H.S., Beak K. ., Structural Control of Cellulose Nanofibrous Composite Membrane with Metal Organic Framework (ZIF-8) for Highly Selective Removal of Cationic Dye, *Carbohyd. Polym.*, **222**:115018(2019).

[11] Singh S., Shang L.L., Srivastava V.C., Hiwarkar A. D., Comparative Study of Electrochemical Oxidation for Dye Degradation: Parametric Optimization and Mechanism Identification, *J. Environ. Chem. Eng.*, **4(3)**: 2911-2921(2016).

[12] Hamoud H.I., Finqueneisel G., Azambre B., Removal of Binary Dyes Mixtures with Opposite and Similar Charges by Adsorption, Coagulation/Flocculation and Catalytic Oxidation in the Presence of CeO_2/H_2O_2 Fenton-like System, *J. Environ. Manage.*, **195(2)**:195-207(2017).

[13] Li X., Hao H.M., Lang X.J., Molecular Design of Dye-TiO2 Assemblies for Green Light-induced Photocatalytic Selective Aerobic Oxidation of Amines, *J. Colloid Interf. Sci.*, **581**(Part B): 826-835(2021).

[14] Palukuru P.S., Devangam A.V., Behara D.K., N, S-Codoped TiO_2/Fe_2O_3 Heterostructure Assemblies for Electrochemical Degradation of Crystal Violet Dye, *Iran. J. Chem. Chem. Eng. (IJCCE)*, **39(2)**: 171-180 (2020).

[15] Mahmoodi N.M., Keshavarzi S., Ghezelbash M., Synthesis of Nanoparticle and Modelling of Its Photocatalytic Dye Degradation Ability from Colored Wastewater, *J. Environ. Chem. Eng.*, **5(4)**: 3684-3689 (2017).

[16] Abharya A., Gholizadeh A., Structural, Optical and Magnetic Feature of Core-shell Nanostructured Fe_3O_4@GO in Photocatalytic Activity, *Iran. J. Chem. Chem. Eng. (IJCCE)*, **39(2)**: 49-58 (2020).

[17] Yusan S., Korzhynbayeva K., Aytas S., Tazhibayeva S., Musabekov K., Preparation and Investigation of Structural Properties of Magnetic Diatomite Nanocomposites Formed with Different Iron Content, *J. Alloy. Compd.*, **608**: 8-13 (2014).

[18] Duan C., Meng X., Liu C. R., Lu W. L., Liu J., Dai L., Wang W.L., Zhao W., Xiong C.Y., Ni Y. H., Carbohydrates-rich Corncobs Supported Metal-organic Frameworks as Versatile Biosorbents for Dye Removal and Microbial Inactivation, *Carbohyd. Polym.*, **222**: 115042 (2019).

[19] Marahel F., Adsorption of Hazardous Methylene Green Dye from Aqueous Solution onto Tin Sulfide Nanoparticles Loaded Activated Carbon: Isotherm and Kinetics Study, *Iran. J. Chem. Chem. Eng. (IJCCE)*, **38(5)**: 129-142 (2019).

[20] Shahsavani S., Dehghani M., Shamsedini N., Removal of Direct Red 81 from Aqueous Solution Using an Acidic Soil Containing Iron (Cade Study of Lahijan Soil), *Iran. J. Chem. Chem. Eng. (IJCCE)*, **38(2)**: 107-112 (2019).

[21] Wang G.H., Liu Q.J., Chang M.M., Jang J.Y., Sui W.J., Si C.L., Ni Y.H., Novel Fe_3O_4@Lignosulfonate /Phenolic Core-shell Microspheres for Highly Efficient Removal of Cationic Dyes from Aqueous Solution, *Ind. Crop. Prod.*, **127**: 110-118(2019).

[22] Zhang L. L., Lu H. L., Yu J., McSporran E., Khan A., Fan Y.M., Yang, Y.Q. Wang Z.G., Ni Y.H., Preparation of High-strength Sustainable Lignocellulose Gels and Their Applications for Antiultraviolet Weathering and Dye Removal, *ACS Sustain. Chem. Eng.*, **7(3)**:2998-3009 (2019).

[23] Naeimi H., Nazifi Z.S., Sulfonated Diatomite as Heterogeneous Acidic Nanoporous Catalyst for Synthesis of 14-aryl-14-H-dibenzo[a,j] Xanthenes under Green Conditions, *Appl. Catal. A: Gen.*, **477**: 132-140(2014).

[24] Sun Z.M., Yao G.Y., Liu M.Y., Zheng S.L., In Situ Synthesis of Magnetic MnFe2O4/Diatomite Nanocomposite Adsorbent and Its Efficient Removal of Cationic Dyes, *J. Taiwan Inst. Chem. E.*, **71**: 501-509 (2017).

[25] Fayza B., Fouad B., Rima M., Youcef B., Water Adsorption and Antibacterial Activity Studies for Characterization of Ca-LTA Zeolite/Diatomite Adsorbents, *Colloid Interface Sci.*, **35**: 100233 (2020).

[26] Yu W.B., Deng L.L., Yuan P., Liu D., Yuan W.W., Liu P., He H.P., Li Z.H., Chen F.R., Surface Silylation of Natural Mesoporous/Macroporous Diatomite for Adsorption of Benzene, *J. Colloid. Interface. Sci.*, **448**: 545-552(2015).

[27] Jiang L., Liu L., Xiao S., Chen J., Preparation of a Novel Manganese Oxide-modified Diatomite and Its Aniline Removal Mechanism from Solution, *Chem. Eng. J.*, **284**: 609-619(2016).

[28] Chen Z.Y., Gao H.W., Yang J.X., PEI@Mg_2SiO_4: An Efficient Carbon Dioxide and Nitrophenol Compounds Adsorbing Material, *RSC. Adv.*, **4**: 33866-33873 (2014).

[29] Yu Y.C., Hu Z.J., Wang Y., Gao H.W., Magnetic SN-functionalized Diatomite for Effective Removals of Phenols, *Int. J. Miner. Process.*, **162**: 1-5(2017).

[30] Jahan M.S., Saeed A., He Z. B., Ni Y.H., Jute as Raw Material for the Preparation of Microcrystalline Cellulose, *Cellulose*, **18**: 451-459(2011).

[31] Liu P., Oksman K., Mathew A. P., Surface Adsorption and Self-assembly of Cu(II) Ions on TEMPO-oxidized Cellulose Nanofibers in Aqueous Media, *J. Colloid Interf. Sci.*, **464**: 175 (2016).

[32] Dai L., Wang Y., Zou X.J., Chen Z.R., Liu H., Ni Y.H., Ultrasensitive Physical, Bio, and Chemical Sensors Derived from 1-, 2-, and 3-D Nanocellulosic Materials, Small, DOI:10.1002/smll.201906567 (2020).

[33] Huo Y.X., Wu H., Wang Z. L., Wang F., Liu Y.L., Feng Y.Y., Zhao Y.N., Preparation of Core/Shell Nanocomposite Adsorbents Based on Amine Polymer-modified Magnetic Materials for the Efficient Adsorption of Anionic Dyes, *Colloid Surface A- Physicochemical and Engineering Aspects*, **549**:174-183(2018).

[34]Lu T.T., Zhu Y.F., Qi Y.X., Kang Y.R., Wang A.Q., Tunable Superporous Magnetic Adsorbent Prepared *via* Eco-friendly Pickering MIPEs for High-efficiency Adsorption of Rb^+ and Sr^{2+}, *Chem. Eng. J.*, **368**:988-998(2019).

[35] Lu H. L., Zhang L.L., Wang B.B., Long Y.D., Zhang M., Ma J.X., Khan A., Chowdhury S.P., Zhou X.F., Ni Y.H., Cellulose-supported Magnetic Fe_3O_4–MOF Composites for Enhanced Dye Removal Application, *Cellulose*, **26**: 4909-4920(2019).

[36] Li Y., Xiao H.N., Chen M.D., Song Z. P., Zhao Y., Absorbents Based on Maleic Anhydride-Modified Cellulose Fibres/Diatomite for Dye Removal, *J. Mater. Sci.*, **49**: 6696 - 6704 (2014).

[37] Al-Degs Y., Khraisheh M.A., Tutunji M.F., Sorption of Lead Ions on Diatomite and Manganese Oxides Modified Diatomite, *Water Res.*, **35(15)**: 3724–3728 (2001).

[38] Zhao H.B., Kwak J.H., Zhang Z.C., Brown H.M., Arey B.W., Holladay J.E., Studying Cellulose Fiber Structure by SEM, XRD, NMR and Acid Hydrolysis, *Carbohyd. Polym.*, **68(2)**: 235-241(2007).

[39] Li J., Wang X.J., Wang J., Li Y., Xia S.Q., Zhao J.F., Simultaneous Recovery of Microalgae, Ammonium and Phosphate from Simulated Wastewater by MgO Modified Diatomite, *Chem. Eng. J.*, **362**: 802-811 (2019).

[40] Zhou J.P., Li R., Liu S. L., Li Q., Zhang L. Z., Zhang L.N., Structure and Magnetic Properties of Regenerated Cellulose/Fe3O4 Nanocomposite Films, *J. Appl. Polym. Sci.*, **111(5)**: 2477−2484(2009).

[41] Kumari S., Chauhan G. S., Ahn J.H., Novel Cellulose Nanowhiskers-based Polyurethane Foam for Rapid and Persistent Removal of Methylene Blue from Its Aqueous Solutions, *Chem. Eng. J.*, **304**: 728-736 (2016).

[42] Alothman Z.A., Ali R., Naushad M., Hexavalent Chromium Removal from Aqueous Medium by Activated Carbon Prepared from Peanut Shell: Adsorption Kinetics, Equilibrium and Thermodynamic Studies, *Chem. Eng. J.*, **184**: 238-247(2012).

[43] Ahamad T., Naushad M., Eldesoky G.E., Al-Saeedi S.I., Nafady A., Al-Kadhi N.S., Al-Muhtaseb A.H., Khan A.A., Khan A., Effective and Fast Adsorptive Removal of Toxic Cationic Dye (MB) from Aqueous Medium Using Amino-functionalized Magnetic Multiwall Carbon Nanotubes, *J. mol. Liq.*, **282**:154-161 (2019).

[44] Dutta D.P., Nath S., Low Cost Synthesis of SiO_2/C Nanocomposite from Corn Cobs and Its Adsorption of Uranium (VI), Chromium (VI) and Cationic Dyes from Wastewater, *J. Mol. Liq.*, **269** :140-151 (2018).

[45] Bharti S.N., Madras G., Adsorption of Anionic Dyes on a Reversibly Swelling Cationic Superabsorbent Polymer, *J. Appl. Polym. Sci.*, **127**: 2251-2258 (2013).

[46] Khalil A., Sergeevich N., Borisova V., Removal of Ammonium from Fish Farms by Biochar Obtained from Rice Straw: Isotherm and Kinetic Studies for Ammonium Adsorption, *Adsorpt. Sci. Technol.*, **36**: 1294–1309(2018).

[47] Yu Q., Xia D., Li H., Ke L., Wang Y., Wang H., Zheng, Y., Li, Q., Effectiveness and Mechanisms of Ammonium Adsorption on Biochars Derivedbfrom Biogas Residues, *RSC Adv.*, **6**: 88373–88381 (2016).

[48] Zhang, X., Lin, X., He, Y., Chen, Y., Zhou, J., Luo, X., Adsorption of Phosphorus from Slaughterhouse Wastewater by Carboxymethyl Konjac Glucomannan Loaded with Lanthanum, *Int. J. Biol. Macromol.*, **119**: 105–115(2018).

[49] He X.Y., Male K.M., Nesterenko P. N., Brabazon D., Paull B., Luong J.H.T., Adsorption and Desorption of Methylene Blue on Porous Carbon Monoliths and Nanocrystalline Cellulose, *ACS Appl. Mater. Inter.*, **5**:8796-8804(2013).

[50] Albadarin A.B., Collins M.N., Naushad M., Shirazian S., Walker G., Mangwandi C., Activated Lignin-chitosan Extruded Blends for Efficient Adsorption of Methylene Blue, *Chem. Eng. J.*, **307**: 264-272(2017).

[51] Dehghani M.H., Dehghan A., Alidadi H., Dolatabadi M., Mehrabpour M., Converti A., Removal of Methylene Blue Dye from Aqueous Solutions by a New Chitosan/Zeolite Composite from Shrimp Waste: Kinetic and Equilibrium Study, *Korean J. Chem. Eng.*, **34(6)**: 1699-1707(2017).

[52] Le M.Q.C., Cao X.T., Lee W.K., Hong S.S., Lim K.T., Fabrication and Adsorption Properties of Novel Magnetic Graphene Oxide Composites for Removal of Methylene Blue, *Mol. Cryst. Liq. Cryst.*, **644(1)**: 160-167(2017).

[53] Mohammadi A., Veisi P., High Adsorption Performance of β-cyclodextrin- functionalized Multi-Walled Carbon Nanotubes for the Removal of Organic Dyes from Water and Industrial Wastewater, *J. Environ. Chem. Eng.*, **6(4)**: 4634-4643(2018).

[54] Zhang S.W., Yang H.C., Huang H.Y., Gao H.H., Wang X.X., Cao R.Y., Li J. X., Xu X. J., Wang X. K., Unexpected Ultrafast and High Adsorption Capacity of Oxygen Vacancy-rich WOx/C Nanowire Networks for Aqueous Pb^{2+} and Methylene Blue Removal, *J. Mater. Chem. A*, **5(30)**: 15913-15922 (2017).

[55] Zhang J., Ping Q.W., Niu M.H., Shi H.Q., Li N., Kinetics and Equilibrium Studies from the Methylene Blue Adsorption on Diatomite Treated with Sodium Hydroxide, *Appl. Clay Sci.*, **83-84**: 12-16 (2013).

[56] Mohamed E.A., Selim A.Q., Zayed A.M., Komarneni S., Mobarak M., Seliem M.K., Enhancing Adsorption Capacity of Egyptian Diatomaceous Earth by Thermochemical Purification: Methylene Blue Uptake, *J. Colloid Interf. Sci.*, **534**:408-419(2019).